

# Predicting insertion: external force application onto cells allow nanowire arrays to insert into cytosol

Nicolai Vanggaard Bærentsen\*, Nina Buch-Månson, and Karen L. Martinez

Received June 2017, Accepted April 2018

The use of vertical nanowires in biosensing application is limited by the extend of how efficient nanowires can reach the intracellular domains. Studies have found nanowire insertion to be successful through single nanowire experiments with high force pr. nanowire, using AFM. This is inadequate for producing high throughput analysis of several cells with multiple nanowires inserting in each cell. Here, we present a model for prediction of the nanowire insertion rates, when centrifugating cell samples down onto arrays of vertical indium arsenide nanowires, with a diameter of 100 nm, height of 3  $\mu\text{m}$  and spacing of 3-5  $\mu\text{m}$ . The model utilizes sedimentation rate of cells in conjunction with the centrifugal force field applied to objects subjected to centrifugation. Various conditions tested with the model, including lowering the temperature of the experiment from room temperature to 4  $^{\circ}\text{C}$ , show that cell viability is not negatively affected by any of the conditions. The insertion rate has been shown to be largely affected by the density of the nanowire array substrate, with a lower density resulting in a higher NW insertion rate, as the model predicts. The percentage of cells with at least one successful nanowire insertion is, however, oppositely affected by density, as a higher density results in larger percentage of cells with successful insertions.

## 1 Introduction

Many scientific applications require entry into the inside of a living cell, with regards to detections of biochemical composition or delivery of larger molecules<sup>1,2</sup>. Vertical nanowires (NWs) are emerging as promising candidates for this task, with the addition of allowing high throughput methods by arranging NWs in highly ordered arrays. NWs have small enough dimensions to penetrate the plasma membrane without causing significant damage to the membrane or the cell<sup>3,4</sup>. Different NWs are currently being used in the field, in many different ways to access the intracellular parts, with varying lengths, diameters, geometric patterns, surface coatings etc. to try to approach the problem in as many ways as possible<sup>2,5-7</sup>. Examples utilizing NWs to study live cells include using a NW on an AFM tip to punch, into the surface of the membrane, gentle seeding of cells on NWs, a NW-based cell endoscope, and electroporation<sup>1,8-14</sup>. In addition to single NW experiments, highly ordered arrays of NWs have been developed, which allows for deeper understanding of cell/NW interaction. Calculations on cell/NW array interaction have shown that indentation can be predicted, since

the difference between cell suspension and NWs indentation depends on whether the energetically gain of cell-surface contact with NWs and substrate can outweigh the cost of a NW invagination<sup>15</sup>. Arrays of NWs have also been used to co-deliver multiple different molecules and proteins into cells simultaneously by co-positioning them on the same NW array<sup>2</sup>. When arrays of NWs are utilized for insertion, as opposed to a single NW, the cell sometimes experience suspension on the NW arrays like tiny fakirs, while the viability of the cells remain unchanged in either condition<sup>15</sup>. Cells cultured on NW arrays of various diameter have shown to survive and proliferate for several days after seeding, though the highest viability rates result from the smallest NW diameter<sup>12</sup>. Furthermore, studies observing cellular health as affected by interaction of different types of NW arrays, show that membrane integrity, enzymatic activity, and other cellular functions have been maintained during NW array exposure, including on Indium Arsenide (InAs) NW arrays, that are used in these experiments<sup>5</sup>. Some publications on experiments of NW arrays as intracellular delivery methods have suggested that there are other factors, than the lipid bilayer, that plays a role in NW insertion, which has lead to the exploration of the cytoskeleton as a factor for penetration<sup>6,12,14,16</sup>. Studies have shown that the elasticity of the membrane, more specifically the actin filaments and mi-

*Bionanotechnology and Nanomedicine Laboratory, Department of Chemistry and Nano-science Center, University of Copenhagen, Universitetsparken 5, DK-2100, Copenhagen, Denmark. \*Corresponding author, e-mail: gc945@alummi.ku.dk*

crotubules, has a great influence on how successful insertion of a NW is<sup>8</sup>. The cytoskeleton protein mesh creates a structure which hardens the membrane and, depending on the cell type, requires a stronger force to indent it; preventing insertion from easily happening<sup>11</sup>. The presence of the cytoskeleton is, however, crucial for successful penetration of the plasma membrane, as studies on liposomes as well as many different cell types with cytoskeletons show that membranes consisting of pure lipid bilayer can not be ruptured by a nanoneedle(NW with a larger diameter)<sup>8</sup>.

The fraction of cells having at least one NW inserted have shown to reach almost 100%, when using a high enough density of NWs, but the fraction of NWs that are inserted remain very low in publications where gravitational force alone acts to insert the NWs<sup>13</sup>. A mechanical model has established that insertion exclusively from gravitational pull only happens in very rare cases, and primarily in setups where the NW diameter is less than 10 nm<sup>17</sup>. Rare cases like this is not adequate for the development of a model for insertion rates, and thus the centrifuge is utilized to increase the force application during interfacing on NW arrays, with the hope that the additional force can lead to better insertion rates.

The theoretical force calculations are based on a model from a previously developed interfacing setup, in the research group, where cells were centrifuged directly down onto a NW array through a swing bucket centrifuge. This allow readily calculating force application on the cells, and adjusting the model in accord with the discoveries. The purpose of this study is to theoretically simulate the centrifugation of cells onto a substrate, and improve the experimental centrifugation based interfacing method. The method uses the consistent force of a centrifuge to force the array of InAs NWs through the cell membrane, as they sediment, and then allow determining viability and insertion in the cells afterwards through fluorescent confocal microscopy and widefield microscopy.

## 2 Materials and methods

**Force calculations.** Cell sedimentation speed ( $V_s$ ) was calculated based on distance from cell to centrifuge ( $r$ ), density of the cell ( $D$ ), viscosity of the medium( $\eta$ ), centrifugal acceleration ( $\omega$ )(Eppendorf 5810R), medium density ( $\rho$ ), cell radius ( $R$ ), and build up speed of rotor (Eppendorf A-4-81). The velocity was evaluated for each 0.01 second to be recalculated based on the new distance to the centrifuge center and new rotor speed. The calculations were made through scripting in Python 2.7, as were the graphics depicting the results.

**Cell culture and preparation.** Mammalian Flp-in™ T-REx™ Human embryonic kidney 293 (HEK293) cells were used as the staple cell line for the experiments, with

a SNAP-TAC domain inserted at the Flp-in site in the plasmid. The SNAP-TAC was expressed upon addition of tetracycline to the media, as the tetracycline acted as a regulator of the active *tet* repressor homo-dimer, by unblocking the transcription of the Flp-in site. For all centrifugation experiments, a special Hyper-DMEM (420 mOsm/L) buffer was used (500 mL Dulbecco's Modified Eagle Medium (DMEM, Gibco), 7.2 g glucose (Sigma) and 10 mM MgCl<sub>2</sub> (Fluka), pH 7.4) to increase the osmolarity of the surrounding medium, in order to reduce the cytoplasmic volume of the cells, leaving the cells with surplus membrane. Prior experiments in the research group (unpublished data) have shown that using Hyper-DMEM promotes NW insertion further, compared to using regular buffer. Hyper-DMEM was only used during the experiments and not as growth medium. The mammalian cells were grown in a T25 culture flasks (Cellstar) in 4 mL 10% Fetal Bovine Serum (FBS, Gibco) in DMEM (growth medium) and split in order to monitor the confluency level. Prior to each centrifugation experiment, and always every 3-4th day, 4 mL of mammalian cell culture was split, by addition of first 2 mL 5 mM EGTA (Invitrogen)(for experiment) or Trypsin-EDTA (Gibco)(for normal splitting) in Phosphate-Buffered Saline (PBS, Gibco) at 37°C for 2 minutes, followed by addition of 2 mL growth medium and subsequent harvesting at 1200 rpm (Eppendorf 5702, Eppendorf A-4-38) for 2 minutes. The cell pellet was resuspended in either 1 mL (for experiments) or 2 mL (for normal splitting) DMEM. For experiments, the cells were counted to ensure a concentration of approx. 350,000 cells pr 50-100  $\mu$ L. For normal cell splitting, 500  $\mu$ L of resuspended cell pellet was transferred to a new culture flask with 3.5 mL 10% FBS in DMEM, 1.5  $\mu$ M Blastidicin(Gibco), 2  $\mu$ M Hygromycin B(Gibco), and left in incubator at 37°C, 5% CO<sub>2</sub> and >95% humidity. The mammalian cells were split in order to prevent too high confluency. Cells were split no later than two days before an experiment, in order to ensure a better separation of living and dead cells, by allowing the live cells time to adhere to the surface of the culture flask.

**Interfacing by centrifugation.** Initial experiments were carried out on glass slides to find suitable conditions for later testing on NWs. A 15 mL falcon tube was filled with 13 mL Hyper-DMEM buffer and adjusted to the correct temperature for the experiment. A glass slide and a fitting polystyrene adapter(custom made at on-site workshop) were washed in 70% EtOH and MQ H<sub>2</sub>O. The glass slide was then inserted into the adapter, to create a flat surface for the cell to hit during experiments, and slowly lowered into the test tube, while keeping the slide in place. The addition of the adapter to the tube brought the combined volum of the contents to the 15 mL mark, and ensured that the cells would travel exactly 8 cm in the test tube, before

reaching the bottom. Approximately 350,000 cells were extracted from the cell culture, equivalent to 50-100  $\mu\text{L}$  depending on the cell growth, and gently pipetted onto the meniscus, followed by immediate centrifugation of the test tube, in order to limit possible premature sedimentation. After centrifugation the adapter, including the glass slide, was gently lifted out of the tube, and the glass slide was placed in a 25 mm petri dish (VWR) with 2 mL Hyper-DMEM and left to rest in at 37 °C for 4 hours. The part of the experiments regarding interfacing was exactly identical for glass slides and NW arrays, with the exception of which substrate was placed in the polystyrene adapter.

**Viability assay.** After 4 hours, three fluorophores were added to the petri dish to allow differentiation between living, dead and total cell count. For mammalian cells centrifuged onto glass slides, the SNAP-TAC was not expressed, instead the cells were dyed with 3  $\mu\text{M}$  Calcein AM (Invitrogen, peak excitation: 495 nm and emission: 515 nm<sup>18</sup>), 6  $\mu\text{M}$  Ethidium homodimer-1 (EthD-1, Invitrogen, peak excitation: 528 nm and emission: 617 nm<sup>19</sup>), and 5  $\mu\text{M}$  DRAQ5 (Biostatus, peak excitation: 600 nm and emission: 697 nm<sup>20</sup>). After staining, the cells were visualized using a wide field microscope (Leica DM 5500, upright fluorescent wide field) with the following filter cubes: GFP (excitation: 470 nm  $\pm$ 40, nm emission: 525 nm  $\pm$ 25 nm) to identify signals from Calcein, Cy3 (excitation: 531 nm  $\pm$ 40 nm, emission: 593 nm  $\pm$ 40 nm) for signals from EthD-1, and Cy5 (excitation: 620 nm  $\pm$ 60 nm, emission: 700 nm  $\pm$ 75 nm) for signals from DRAQ5. Image analysis was conducted using ImageJ freeware.

**Nanowire penetration assay.** For experiments with NW arrays, 20  $\mu\text{L}$  tetracycline (0.5% volume)(Sigma) was added to the 4 mL cell culture, to initiate the expression of the SNAP-TAC, approximately 24 hours before use. During the resting period after centrifugation, an additional 10  $\mu\text{L}$  tetracycline was added to the 2 mL Hyper-DMEM to keep the expression of the SNAP-TAC at a high level. After 5 hours of resting time, the NW chip was moved from the petri dish to an 8-well  $\mu$ -slide chamber (Ibidi) containing 300  $\mu\text{L}$  Hyper-DMEM and 5  $\mu\text{M}$  SNAP-Surface 649 dye (New England Biolabs, excitation: 655 nm, emission: 676 nm<sup>21</sup>), in order to attach the dye to the SNAP-tag, and left at 37 °C. After 30 minutes, the NW array chip was washed twice with Hyper-DMEM, and transferred to a microscope chamber pre washed with 70% EtOH and MQ H<sub>2</sub>O, containing 300  $\mu\text{L}$  Hyper-DMEM, 3  $\mu\text{M}$  calcein AM and 6  $\mu\text{M}$  EthD-1. The microscope chamber was rested for 5 minutes in darkness, to shield the fluorophores and to let the dyes bind, before visualization on the wide field microscope, for viability images, and inverted confocal microscope (Leica TCS SP5), for NW insertion detection. The settings for the confocal microscope were: 8 bit, 400 Hz, bidirectional scan, zoom 5, z-step 0.17  $\mu\text{m}$ ,

between stacks. The specific laser settings for the different inspections were as follows: For surface and NW: HeNe 633 nm at 3%, reflection 623-643 nm, variable gain. For Calcein: Argon (0%) 488 nm at 3%, emission 508-540 nm, variable gain. For SNAP-Surface 649: HeNe 633 nm at 20%, emission 653-750 nm, gain 1000 V, line average 4. Image analysis was conducted using ImageJ freeware.

### 3 Results

The experimental results were obtained by centrifugation cells onto a flat glass slide through 8 cm of buffer in a test tube (Figure 1). After centrifugation the glass slide was incubated at 37 °C for 4-5 hours followed by staining and counted to test viability. Following the data analysis the experiment conditions were optimized and conducted using nanowire (NW) arrays, instead of glass slides, to test for insertion efficiency.

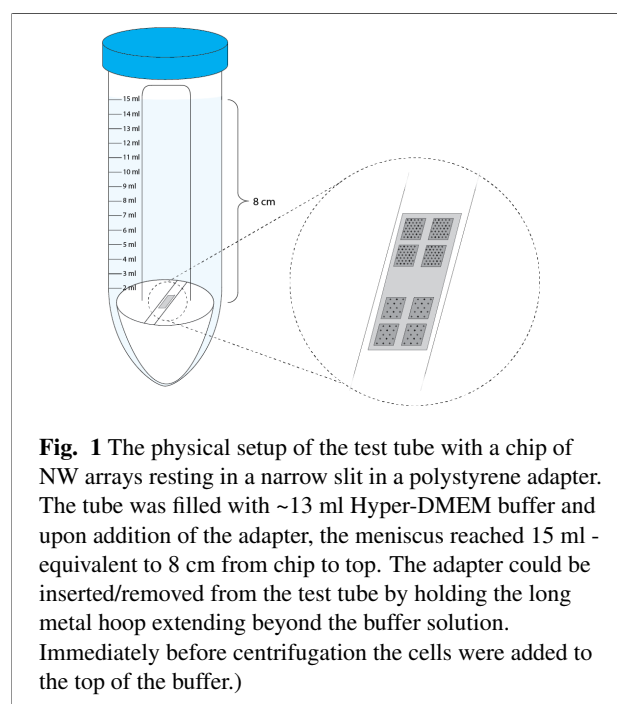


**Fig. 1** The physical setup of the test tube with a chip of NW arrays resting in a narrow slit in a polystyrene adapter. The tube was filled with ~13 ml Hyper-DMEM buffer and upon addition of the adapter, the meniscus reached 15 ml - equivalent to 8 cm from chip to top. The adapter could be inserted/removed from the test tube by holding the long metal hoop extending beyond the buffer solution. Immediately before centrifugation the cells were added to the top of the buffer.)

#### Calculations of force application

In order to achieve the best possible insertion rate of NWs into the cells, the force applied onto the cells have to be maximized as (Berthing *et al*, 2012)<sup>22</sup> showed that gravitational force application alone is insufficient when it comes to penetration of the cell surface. As such, increasing the force between NW and cell surface was suspected to reduce the majority of failed membrane and cytoskeleton penetrations. The insertion rate was tested theoretically in two phases: first by calculating the velocity of cells during

centrifugation in the setup available and second by calculating how the parameters of the centrifuge available affects the total centrifugation time.

### Velocity of cells during centrifugation

In order to produce a sensible model for NW insertion into cells, calculations on the cell sedimentation rate, and its dependencies, was performed by following (Katkov *et al*, 1999)<sup>23</sup>, using the function for calculating sedimentation velocity of a cell:

$$v_s = \frac{2R^2 \cdot (D - \rho) \cdot \omega^2 \cdot r}{9\eta} \quad (1)$$

where  $v_s$  is the velocity of the cell,  $R$  is the radius of the cell,  $D$  is the density of the cell,  $\rho$  is the density of the medium,  $\omega$  is the angular velocity of the rotor,  $r$  is the distance from the cell to the center of the rotor, and  $\eta$  is the viscosity of the medium (DMEM)(Bacabac *et al*, 2005)<sup>24</sup>. The angular velocity is a function of time and can be calculated as  $\omega(t) = \frac{t}{34} \cdot \omega_{\max}$ , as the centrifuge takes 34 seconds to reach max speed of ~440 radians/second(3000 G). The distance travelled by the cells is calculated after each 0.01 second, based on the velocity of the cells and the velocity of the rotor as it builds up its speed. A graph depicting the velocity of the cell sample during centrifugation as a function of time was made by simulations in Python shown in Figure 2. From the data points of the graph, the time of impact at  $t_{R=0.15m}$ , can be calculated as the sum of the velocity  $v_s$  times 0.01 second per iteration  $n$  until the sum = 0.08 m. This will show at which iteration the cells have travelled the 8 cm in the test tube, and be at the 15 cm mark, as they start 7 cm from the center of the rotor. The procedure is similar to integrating the function of the curve, but in this case more precise since a regression function would be needed. The calculations show impact time to be 23.43 seconds or about 2/3 of the time the centrifuge takes to reach max velocity ( $\omega$ ), meaning that the cells reach the bottom even before the centrifuge is at full speed.

The model shown in Figure 2 assumes no sedimentation prior to centrifugation initiation, a practically impossible scenario, and the sedimentation time is therefore likely to be affected and thereby slightly lower.

The centrifuge parameters tested for effects on the final centrifugation time were the maximum angular velocity of the centrifuge, the maximum distance from the center of the rotor that the cells can reach, and the build up speed of the centrifuge.

Plotting time needed to reach the bottom as a function of two of the three parameters with the remaining being at the default setup, shows how each parameter influences the time in the setup (Figure 3). Faster centrifugation time results in most cases, in higher velocity and greater force

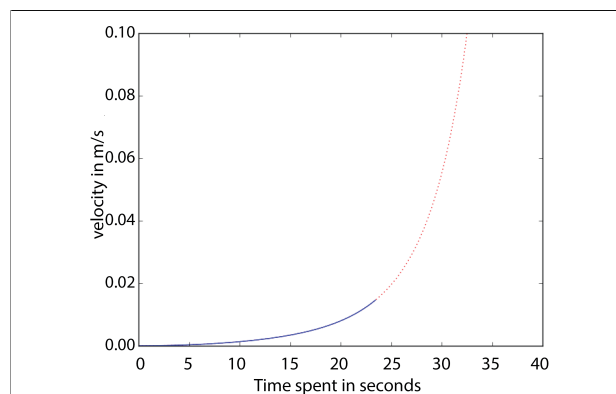
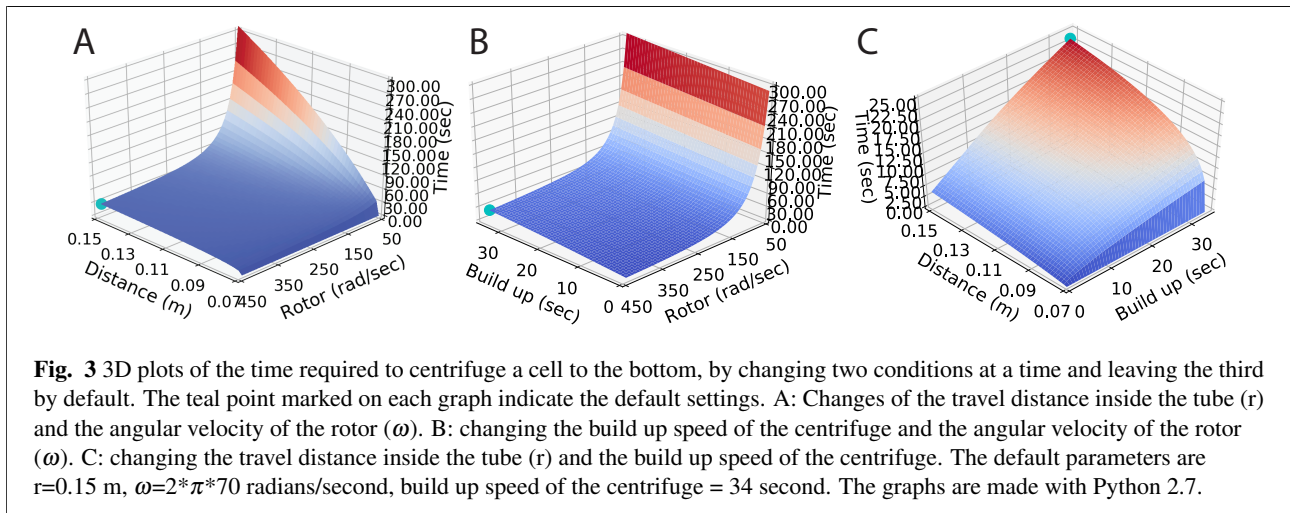


**Fig. 2** The graph depicts the velocity of cells vs time. The blue line represents the segment of the speed reached by the cells in the possible setup with the centrifuge, which means a max final distance of 15 cm. The red line represents the theoretical propagation assuming an infinitely deep tube. The graph is made using Python 2.7. y-axis: velocity (m/s); x-axis: time (s)

exerted on the cells, with the exception of near-zero results where the short centrifugation time is more likely attributed to the miniscule travel distance. As seen in Figure 3A the change in either final distance travelled or angular velocity does not appear to significantly affect the time required in the regime of the default setup. Figure 3B does however indicate that build up time of the centrifuge lowers the time spend from ~20 seconds to <10 seconds build up. For both Figure 3A+B the time scale is significantly larger than the time scale for Figure 3C due to the major impact from the angular velocity of the rotor in the low regime <150 radians/second. The build up time parameter is seen as having the greatest impact on centrifugation time and thus cell velocity at impact, as can be seen in Figure 3C. Going from 34 seconds in the default setup to optimally 0 seconds decreases the time spend by more than a factor 5, and with an almost linear effect on the time, a relative change to the default setup would bring the greatest impact to time spent.

From the above calculations, it appears that the cells can reach the bottom of the test tube significantly faster than previous experiments conducted in the research group assumes(unpublished data), where a 120 second centrifugation time was employed. To test if centrifugation time has any influence, and how great it possibly is, a setup with a glass slide was tested to see the effect on viability. In case this showed a constant amount of cells, the calculations on sedimentation time would be confirmed. A set of values was determined to be used in the following experiments, where one or two were varied at a time. They will subsequently be referred to as the default parameters (end distance from rotor = 15 cm, angular velocity of the rotor =  $2 \cdot \pi \cdot 70$  or approximately 440 radians/second (3000 G),





build up speed = 34 seconds and centrifugation time = 60 seconds). After analyzing the effects, if any, centrifugation time has on cell viability and availability at the bottom, the best parameters were chosen for NW array insertion experiments, where the parameters were evaluated to optimize insertion efficiency.

### Viability tests on glass slides

The viability tests were made by centrifugation of a droplet of cells onto a glass slide resting as a flat surface on the adapter inside the test tube (Figure 1). The cell line employed was a Flp-in T-REX HEK293 stable cell line, which was dyed using calcein AM and ethidium homodimer 1 (EthD-1) and DRAQ5. The images were produced with a wide field microscope, using GFP, Cy3 and Cy5 (data not shown) filter cubes. All assays using the glass slide substrate were tested using the default parameters, but with varying centrifugation time. The experiments on glass slides were carried out at two different centrifugation times, one at 120 seconds as a reference point and upper margin, as this was the centrifugation time at which all previous experiments in the research group had been conducted at, and one 60 seconds to see whether it could lead to any significant differences (Figure 4A+B). An increase in cell viability at 60 seconds compared to 120 seconds (77.77% survival for 60 seconds vs 69.32% survival for 120 seconds) was observed (Table 1). Because of this another experiment with 30 seconds of centrifugation time was conducted to investigate whether this tendency would continue even at shorter centrifugation times. The cells were also centrifuged for 60 seconds as a control in this experiment, to be able to directly compare the state of the cells relative to the previous experiment. Even though cell viability after 60 seconds of centrifugation time decreased in the second experiment, compared to the first experiment, the relative cell viability after 30 seconds of centrifugation

was still higher (Figure 4C+D, 75.12% survival for 30 seconds vs 71.81% survival for 60 seconds). Assuming the average cell viability for 60 second centrifugation time lying somewhere in between the two measurements, and the cell viability at 30 and 120 seconds are adjusted accordingly, there is clearly a change between 30, 60 and 120 seconds of centrifugation time. The viability tests

**Table 1** The viability of the cells from two individual experiments, the first conducted at 60 and 120 seconds, and the second conducted at 30 and 60 seconds. The cells were centrifuged onto glass slides, using the default parameters with varying centrifugation time, to test the effect of centrifugation time as well as impact force on the viability of the cells.

Experiment/ centrifugation time (sec)	30	60	120
1		77.77%	69.32%
2	75.12%	71.82%	

of glass slides show that centrifugation time has some influence on the viability of the cells, but is most likely not the difference between the results as seen and a 100% survival rate, since changing from 120 seconds to 30 seconds only resulted in ~10% more surviving cells. This suggests that, of the two conditions tested, initial impact is probably the greater contributor towards cell death rather than prolonged exposure to centrifugation. From the images of the viability experiments it appears that the shorter centrifugation times (Figure 4C+D) effects to total amount of cells reaching the bottom. For each experiment eight wide field microscope images were taken at various locations on the glass slide, to provide an average result of the cell density and viability. For the first experiment, the average amount of cells that reached the bottom, that is the total cell count on each image, for the 60 second and 120 second tests had less than 1% variation between them (data not shown). For the second experiment, with centrifugation times of 30

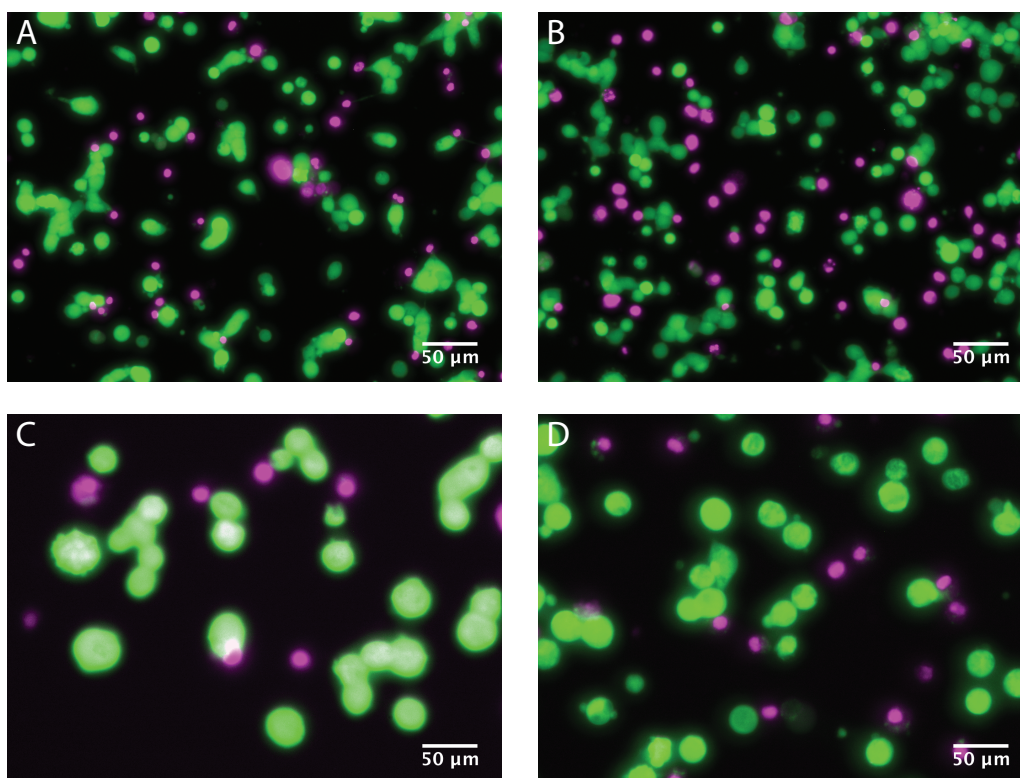


**Fig. 4** Viability tests of cells centrifuged onto glass slides using the default conditions and varying centrifugation time. The green channel show the living cells dyed with 3  $\mu\text{M}$  Calcein AM, and the magenta channel show dead cells dyed with 6  $\mu\text{M}$  EthD-1. The nuclei of the cells were also colored using DRAQ5 (data not shown), to ensure that the total cell count was within a reasonable margin of the living and dead combined. (A) experiment 1 at 60 seconds; (B) experiment 1 at 120 seconds; (C) experiment 2 at 30 seconds; (D) experiment 2 at 60 seconds. Images were obtained with wide field microscopy, using GFP and Cy3 filter cubes. In all four images it is clear that the amount of living cells outnumber the dead by a large ratio.

seconds and 60 seconds, the variation was 18% (data not shown). The difference in average cell count between the two sets of experiments is however a factor 5-7. This suggests, that even though there is a significant change in the total amount of cells at 30 seconds and 120 seconds, and the two 60 second experiments, the difference originates not from centrifugation time but rather from the amount of cells used in the two experiments. Therefore cell death is most likely caused by multiple factors, including some that are not directly related to these experiments. Dead cells were only removed from the cell culture before splitting when all living cells adhered to the surface, and thus any treatment thereafter producing dead cells was unavoidable, such as the slower centrifugation at 1200 rpm ( $\sim 20$  radians/second) during harvest of the cells for the experiment. Based on the initial calculations and the viability tests on the glass slides, the centrifugation time for the NW arrays was set to 60 seconds, as 120 seconds would increase the risk of cell death and 30 seconds might be too short if the effect of continuous exposure had any influence on the insertion rate.

#### Nanowire insertion assay using arrays of equally spaced nanowires

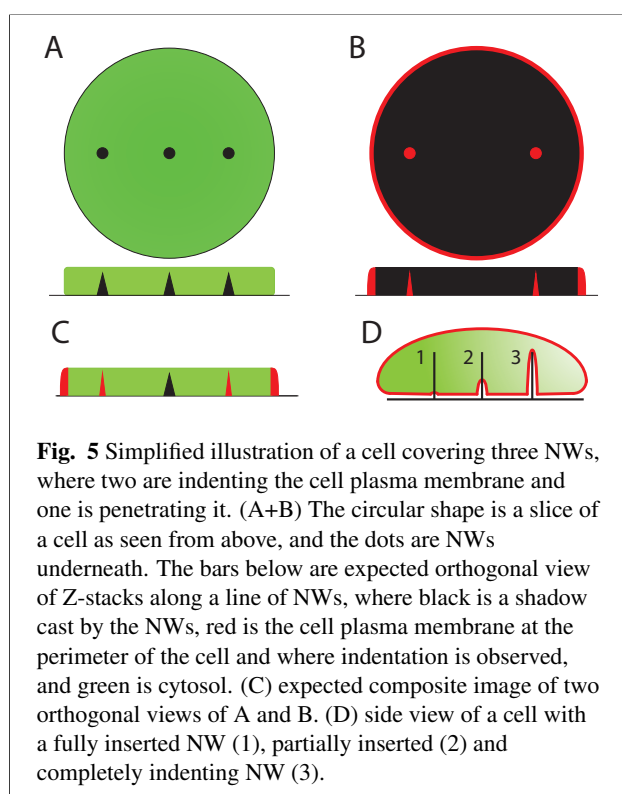
For the NW insertion assay, the HEK 293 cell line had their SNAP-TAC expressed, to allow binding of the SNAP-Surface 649 dye used. The dye tag, is attached to the TAC part, which has a transmembrane helix anchoring the complex in the membrane. The expression of SNAP-TAC is initiated upon addition of tetracycline, which binds a *tet* repressor homodimer upstream of the flip-in site causing the repressor to disengage and allow for transcription of the gene,  $\sim 24$  hours before use. The SNAP-tag binds SNAP-Surface 649 dye which labels the membrane and the cytosol is stained with calcein AM. The calcein AM enters viable cells due to the hydrophobicity of the AM derivative, then once inside the cytosol, intracellular esterases cleave the AM groups off of the non-fluorescent calcein AM, leaving fluorescent calcein inside. Only viable cells have active esterases and thus dead cell will not produce the fluorescence. The resulting images were produced on an inverted confocal microscope as a series of Z-stack images made on various locations of the chip. Along lines of

NWs under the cells, the Z-stacks were inspected orthogonally to see the effect of NWs in the cell. The arrays used consisted of NWs arranged in an isometric pattern with either 3  $\mu\text{m}$  or 5  $\mu\text{m}$  between each NW. These will hereafter be referred to as 3  $\mu\text{m}$  and 5  $\mu\text{m}$  density. All array chips originated from the same batch and all of its NWs were 3  $\mu\text{m}$  high with a diameter of 100 nm. Figure 5 show the anticipated effect of NW insertion in a cell through detection of calcein (Figure 5A) and SNAP-Surface 649 dye (Figure 5B). The calcein dye only functions in live cells, and is not visible when a NW is taking up space as it eliminates the fluorescent signal. As such all NWs should, however indirectly, be visible as a shadow against the signal, and this is used as a reference to verify whether a NW is present or not. The SNAP-Surface 649 dye binds to the surface of the SNAP-TAC on the membrane and should show the perimeter of the cell as well as any NWs that deform the surface to wrap around it, however the signal is not visible if the NWs penetrate the plasma membrane. Figure 5C show the expected composite image, where the shadows in the calcein signal verify the presence of a NW inside the cytosol, and the SNAP-Surface 649 signal show NWs that have indented but not penetrated the surface. According to

onto the cells was calculated with conditions at the time of impact with the default setup, and under the assumption that the cell has a spherical volume. The centrifugal net force on the cell is given by:

$$F = m * \omega(t)^2 * r \quad (2)$$

where F is force, m is mass of the cell,  $\omega(t)$  is the angular velocity of the rotor at impact time t, and r is the distance from impact point to the center of the rotor. Here F is calculated to be 16.9 nN or approximately a factor 10 larger than the documented requirement for a single penetration, meaning that cells covering just 10 NWs or more are likely to have high rates of penetration failure.



(Xie *et al.*, 2013)<sup>17</sup> the force required for successful insertion is  $\sim 1.78$  nN for a single nanostructure (with a diameter of 50 nm) on an AFM-tip, indicating that a denser array of NWs would lead to less successful insertion rate, as the force is distributed onto several NWs. The force exerted

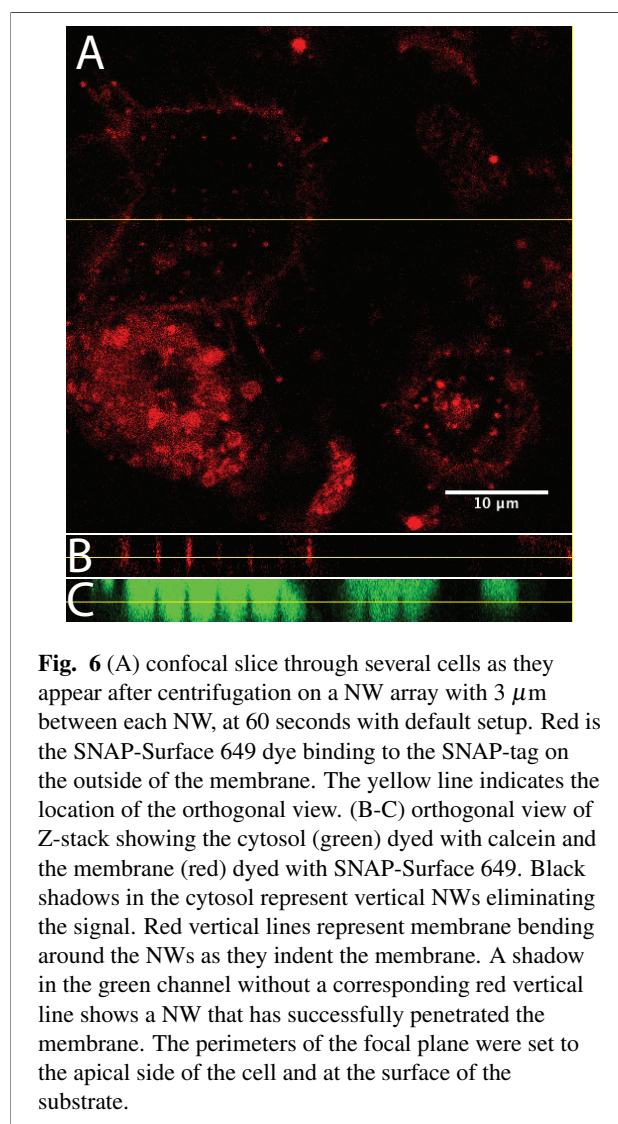


Figure 6A shows a visual cut-through of a cell that covers more than 30 NWs but still has some NWs that are successfully inserted into the cell. Figure 6B-C shows the orthogonal view through the z-axis at the position indicated with the yellow line, and the green calcein signal



**Table 2** Counted data from two experiments (RT, 60 seconds and 4 °C, 60 seconds) as well as data from a previous unpublished experiment from the research group (RT, 120 seconds). The counts represent a sum of 6-10 images of cells and account for the amount of NWs covered by each viable cell in the images as well as the amount of NWs that have successfully or partially inserted into the cell. Each row show a different condition with the corresponding insertion efficiency, how many cells had at least one NW inserted and how many NWs were covered by a cell on average.

Density ( $\mu\text{m}$ ), temperature and time (seconds)	NW covered	NW inserted	% NW insertion	% cells inserted	wires/cell (avg.)
3, RT, 60	223	25	10.00%	56.25%	15.5
5, RT, 60	82	11	11.83%	31.25%	2.90
3, 4°C, 60	107	5	4.46%	30.77%	8.86
5, 4°C, 60	7	1	12.50%	16.67%	1.14
3, RT, 120			8.15% ( $S_E=1.35$ )	62.28% ( $S_E=8.45$ )	
5, RT, 120			13.81% ( $S_E=5.00$ )	57.98% ( $S_E=6.84$ )	

with shadows cast by the NWs as expected. The red membrane signal however shows that insertion has failed for the majority of the NWs, in accordance with the expectations. Cells on the 3  $\mu\text{m}$  spacing arrays cover anywhere from 10 to +30 NWs with an average of 13.75 NWs, whereas the 5  $\mu\text{m}$  spacing arrays only has cells covering less than 10 NWs with an averaging of 3.36 NWs. Both 3  $\mu\text{m}$  (Figure 6A) and 5  $\mu\text{m}$  (data not shown) density show cells with NWs inserted, with a larger fraction inserted with the 5  $\mu\text{m}$  spacing (Table 2), as expected from the calculations. However, the difference in total amount of NWs inserted could also originate from a difference in the amount of NWs present under the cells. An increase in sheer numbers would potentially increase the number of insertions, until a certain density is reached at which point the NWs act as a flat surface to the membrane, or the force is diluted too much by the distribution on a denser NW array. The percentage of cells with at least one NW inserted is significantly higher for 3  $\mu\text{m}$  density compared to 5  $\mu\text{m}$  density arrays and the total amount of successful insertions follow the same trend. This suggests that the density of successful insertions are equally spread on the available cells in both 5  $\mu\text{m}$  density and 3  $\mu\text{m}$  density NW arrays. This means that the rate of cells with successful insertion is governed by the amount of NWs and not the density of the NW arrays.

### Nanowire assay at 4 °C

According to (Kawamura *et al.*, 2016)<sup>10</sup>, lowering the temperature to 4 °C should increase the insertion rate, by rigidifying the membrane. Therefore, an experiment was set up, with the temperature of the cells and the medium reduced to 4 °C prior to centrifugation, to see if this would create a more stiff membrane, allowing for higher rates of insertion. Figure 7 shows three cells where the orthogonal view is taken from the yellow line, and shows that the NWs are all deforming the membrane and failing to insert into the cells. At 4 °C, the 3  $\mu\text{m}$  density has an insertion rate that

is approximately half of that of the RT (room temperature ~25°C) experiment, which could be influenced by the reduced number of NWs, as the amount of NWs covered by each cell is also approximately half of that for the RT experiment. Subsequent investigations of the chips showed that, especially on the 5  $\mu\text{m}$  density arrays, several NWs were missing so that no cells were found to cover more than one NW, thus de facto mimicking an infinitely low density. The same issue was also partially observed for the 3  $\mu\text{m}$  density arrays, where the fraction of missing NWs only affected the density in certain areas below the cells as the cells spanned a much higher number of NWs. For the two 5  $\mu\text{m}$  arrays, the average number of NWs covered by each cell is less than half at 4 °C but unlike the 3  $\mu\text{m}$  arrays, the % NW insertion rate is slightly higher (Table 2), probably due to the low availability of NWs in the 5  $\mu\text{m}$  array, leading to statistical anomalies. Ideally, the insertion rate would be higher when the array density get smaller, as the force is distributed on only one wire instead of many. The NW arrays were also observed in the fluorescence widefield microscope to see if the presence of the NWs would change the death rate of the cells. Both experiments (Table 3) show a survival rate of ~75-80%, at RT and 4 °C, indicating that neither the NW nor the colder environment had any significant influence on the viability of the cells during centrifugation as compared to the glass slides experiments at 60 seconds (Table 1). From table 4

**Table 3** The viability rates of cells from the experiments on the 3  $\mu\text{m}$  density NW arrays. Both experiments were centrifuged for 60 seconds.

NW array, RT	79.10%
NW array, 4°C	77.73%

it can be seen that across all results from the 60 second experiments, a tendency towards single NW penetration is evident. The lack of statistical variation in the number of NWs inserted in each cell is clearly expressed, as the



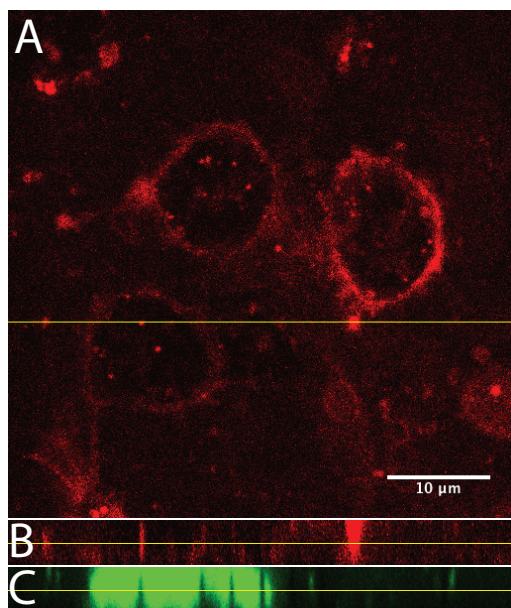


**Fig. 7** (A) confocal slice through several cells as they appear after centrifugation on a NW array with  $3\ \mu\text{m}$  between each NW, at 60 seconds,  $4\ ^\circ\text{C}$ , with default setup. Red is the SNAP-Surface 649 dye binding to the SNAP-tag on the outside of the membrane. The yellow line indicates the location of the orthogonal view. (B-C) orthogonal view of Z-stack showing the cytosol (green) dyed with calcein and the membrane (red) dyed with SNAP-Surface 649. Black shadows in the cytosol represent vertical NWs eliminating the signal. Red vertical lines represent membrane bending around the NWs as they indent the membrane. A shadow in the green channel without a corresponding red vertical line shows a NW that has successfully penetrated the membrane. The perimeters of the focal plane were set to the apical side of the cell and at the surface of the substrate.

number of cells with NWs inserted for each condition only includes 5-11 cells. For the  $4\ ^\circ\text{C}$  experiment, just one additional cell with two or three NWs inserted would change the percentage of both cells that have NWs inserted, and the rate of NWs inserted, by quite a bit. As such the distribution of inserted NWs on different cells are quite different from the 120 second setup because of the relatively few data points.

## 4 Discussion

From the results it is observed that the centrifugation time is determining the viability of the cells when centrifuged on both glass slides and NW arrays. However, the time merely changes the fraction of dead cells by a few percent rather than produce an all or nothing scenario. The tests on NW arrays show that at both RT and  $4\ ^\circ\text{C}$  are the NWs

**Table 4** Calculated data from two produced experiments (RT, 60 seconds and  $4\ ^\circ\text{C}$ , 60 seconds) as well as data from a previous unpublished experiments in the group (RT, 120 seconds). The calculations show the distribution of inserted NWs inside cells with at least one NW.

Density ( $\mu\text{m}$ ), temperature and time(seconds)	1 NW	2 NWs	+3 NWs
3, RT, 60	73%	0%	27%
5, RT, 60	82%	18%	0%
3, $4\ ^\circ\text{C}$ , 60	40%	0%	60%
5, $4\ ^\circ\text{C}$ , 60	100%	0%	0%
3, RT, 120	32%	22%	46%
5, RT, 120	75%	14%	11%

inserted into the cells, though the primary data would suggest that insertion at  $4\ ^\circ\text{C}$  is somewhat lower compared to RT. The difference in insertion rate between  $3\ \mu\text{m}$  and  $5\ \mu\text{m}$  follows the hypothesis that a lower density leads to larger force application per NW and thus a higher insertion rate.

Comparison of insertion rate and cell penetration with previous experiments from the research group, using the same setup but with different centrifugation time shows how this parameter affects the results (Table 2). NW insertion rate for both  $3\ \mu\text{m}$  and  $5\ \mu\text{m}$  at 120 second centrifugation time appear in the same range as the tested values, except for the  $4\ ^\circ\text{C}$   $3\ \mu\text{m}$  result which is off by about a factor 2, suggesting that prolonged centrifugation has a mild or no effect on insertion when it comes to RT experiments.

Since the centrifugation time is observed to only slightly affect the insertion rate, but to have a clear relation to cell death, centrifugation time is thus a less important factor in determining the optimal conditions. This means the data supports the original hypothesis that the initial impact of the cells is the primary cause for NW insertion. The variation however, in number of cells with at least one NW inserted is significantly greater across all experiments with the highest percentage for both  $3\ \mu\text{m}$  and  $5\ \mu\text{m}$  at the 120 second experiments. It can be deduced that even though the same fractions of NWs are inserted into cells, the fact that the actual successful insertions are spread out on many cells, can hardly be attributed to the increased centrifugation time.

From the experiment conducted at  $4\ ^\circ\text{C}$  it is seen that fewer cells have NWs inserted, and at least for  $3\ \mu\text{m}$  density, there is also a lower fraction of all NWs that are inserted. The low temperature has likely had the desired effect of making the cytoskeleton more rigid, but also the undesired effect of hardening the cell membrane as a whole, which explains the low rate of cells with NWs inserted. This could probably be countered by an increase in applied force through speed up of the centrifuge. (Kawamura *et al*, 2016)<sup>10</sup> found that cooling the cells would increase inser-

tion rate when tested with AFM, but in their experiments, they used a single tip along with a force of 40 nN to rupture the plasma membrane at a single location, which is quite far from anything that have been tested here; indeed the closest setup is the 5  $\mu\text{m}$  array that had an insertion rate of 12.5%, similar to the results from the RT tests. To provide a definite conclusion on whether 4 °C has a positive effect on insertion, using our conditions, more independent experiments would have to be conducted.

The results used from the 120 second setup are collected based on a much larger data sets and therefore represent a greater statistical confidence. This also becomes clear from the arrangement of the NW insertion across the different cells.

(VanDersarl *et al*, 2012)<sup>5</sup> found that the success rate for nanostraw insertion through cell suspension was effectively seen to be 1-10% per nanostraw, and even as their setup had ~10-100 nanostraws of diameter >100 nm under each cell, they recorded a success rate of cell penetrated to be 40-70%. This could suggest that that a very high density array can still allow a high rate of cells with successful insertions.

## 5 Conclusion

In summary, this paper uses theoretical force calculations from a centrifuge acting on a cell sample, in conjunction with methods from recent publications to predict the effect of externally applied forces on cells as they sediment on arrays of NWs. The calculations predict that lower array densities will have greater chance of successfully penetrating the cell plasma membrane, as is indeed observed for experiments conducted at both 4 °C and RT. The effect of lowering the temperature of cells and medium to 4 °C does however not appear to positively affect the rate of NW insertion in general. Viability tests conducted at different centrifugation times, and with both NW arrays and glass slides as substrates show that cell viability is not affected by the presence of a NW array compared to a glass slide. It does however show that between prolonged centrifugation and initial impact the latter is the greater contributor to cell death, since centrifugation only had a minor impact of the viability. Based on the results showing that centrifugation time only has minor influence on NW insertion, and that initial impact seems to follow the theoretical model for force application, it is safe to say that initial impact very well could be the major cause for successful NW insertion, as originally suggested.

## 6 Acknowledgements

I would like to thank Bogdan Cristinoi and Nikolaj K. Brinkenfeldt for any help provided making the experi-

ments for this paper.

## References

- 1 C. Xie, Z. Lin, L. Hanson, Y. Cui and B. Cui, *Nature nanotechnology*, 2012, **7**, 185–190.
- 2 A. K. Shalek, J. T. Robinson, E. S. Karp, J. S. Lee, D.-R. Ahn, M.-H. Yoon, A. Sutton, M. Jorgolli, R. S. Gertner, T. S. Gujral, G. MacBeath, E. G. Yang and H. Park, *PNAS*, 2010, **107**, 1870–1875.
- 3 L. Lacerda, S. Raffa, M. Prato, A. Bianco and K. Kostarelos, *Nano today*, 2007, **2**, 38–43.
- 4 S. Bonde, T. Berthing, M. H. Madsen, T. K. Andersen, N. Buch-Månso, L. Gu, X. L. F. Badique, K. Anselme, J. Nygård and K. L. Martinez, *A S C Appl. Mater. Interfaces*, 2013, **5**, 10510–10519.
- 5 J. J. VanDersarl, A. M. Xu, and N. A. Melosh, *Nano letters*, 2012, **12**, 3881–3886.
- 6 T. Berthing, S. Bonde, C. B. Sørensen, P. Utko, J. Nygård and K. L. Martinez, *Small*, 2011, **7**, 640–647.
- 7 T. E. McKnight, A. V. Melechko, G. D. Griffin, M. A. Guillorn, V. I. Merkulov, F. Serna, D. K. Hensley, M. J. Doktycz, D. H. Lowndes and M. L. Simpson, *Nanotechnology*, 2003, **14**, 551–556.
- 8 H. Kagiwada, C. Nakamura, T. Kihara, H. Kamiishi, K. Kawano, N. Nakamura and J. Miyake, *Wiley-Liss*, 2010, **67**, 496–503.
- 9 I. Obataya, C. Nakamura, S. Han, N. Nakamura and J. Miyake, *Nano Letters*, 2005, **5**, 27–30.
- 10 R. Kawamura, K. Shimizu, Y. Matsumoto, A. Yamagishi, Y. R. Silberg, M. Iijima, S. Kuroda and K. Fukazawa, *Journal of Nanobiotechnology*, 2016, **14**, 1–9.
- 11 A. Aalipour, A. M. Xu, S. Leal-Ortiz, C. C. Garner and N. A. Melosh, *Langmuir*, 2014, **30**, 12362–12367.
- 12 W. Kim, J. K. Ng, M. E. Kunitake, B. R. Conklin and P. Yang, *J. Am. Chem. Soc. communication*, 2007, **129**, 7228–7229.
- 13 A. M. Xu, A. Aalipour, S. Leal-Ortiz, A. H. Mekhdjian, X. Xie, A. R. Dunn, C. C. Garner and N. A. Melosh, *Nature communications*, 2014, **5**, 1–8.
- 14 R. Yan, J.-H. Park, Y. Choi, C.-J. Heo, S.-M. Yang, L. P. Lee and P. Yang, *Nature nanotechnology*, 2011, **7**, 191–193.
- 15 N. Buch-Månson, S. Bonde, J. Bolinsson, T. Berthing, J. Nygård and K. L. Martinez, *Advanced functional materials*, 2015, **25**, 3246–3255.
- 16 J. T. Robinson, M. Jorgolli, A. K. Shalek, M.-H. Yoon, R. S. Gertner and H. Park, *Nature nanotechnology*, 2012, **7**, 180–182.
- 17 X. Xie, A. M. Xu, M. R. Angle, N. Tayebi, P. Verma, and N. A. Melosh, *Nano letters*, 2013, **13**, 6002–6008.
- 18 [\url{https://www.bdbiosciences.com/ds/pm/tds/564061}](https://www.bdbiosciences.com/ds/pm/tds/564061), last visited, 30.05.17, 21.00.
- 19 [\url{https://www.thermofisher.com/order/catalog/product/E1169}](https://www.thermofisher.com/order/catalog/product/E1169), last visited, 23.05.17, 11.00.
- 20 [\url{www.biostatus.com/site/biostatus/documents/DR5.TDS003040714.pdf}](http://www.biostatus.com/site/biostatus/documents/DR5.TDS003040714.pdf), last visited, 01.06.17, 22.00.
- 21 [\url{https://www.neb.com/products/s9159-snap-surface-649}](https://www.neb.com/products/s9159-snap-surface-649), last visited, 23.05.17, 11.00.
- 22 T. Berthing, S. Bonde, K. R. Rostgaard, M. H. Madsen, C. B. Sørensen, J. Nygård, and K. L. Martinez, *Nanotechnology*, 2012, **23**, 0–0.
- 23 I. L. Katkov, and P. Mazur, *Cell Biochemistry and Biophysics*, 1999, **31**, 231–245.
- 24 R. G. Bacabaca, T. H. Smith, S. C. Cowinc, J. J. V. Loona, F. T. Nieuwstadt, R. Heethaarb and J. Klein-Nulend, *Journal of Biomechanics*, 2005, **38**, 159–167.